CNR and CO Insertion Reactions of 2,6-Xylyl Isocyanide with *p*-Chlorobenzylpentacarbonylmanganese

Thomas M. Becker,[1a] John J. Alexander,*[,1a] Jeanette A. Krause Bauer,[1a] Jeffrey L. Nauss,[1b] and Fred C. Wireko[1c]

Department of Chemistry, University of Cincinnati, P.O. Box 210172, Cincinnati, Ohio 45221-0172, Molecular Simulations Inc., 9685 Scranton Road, San Diego, California 92121, and The Procter and Gamble Co., Miami Valley Laboratories, 11810 E. Miami River Road, P.O. Box 398707, Cincinnati, Ohio 45239-8707

Received May 17, 1999

Stirring a solution of $(CO)_5MnCH_2C_6H_4$-*p*-Cl, **1**, with 2 equiv of 2,6-xylyl isocyanide in toluene in the presence of a catalytic amount of PdO produced isocyanide insertion products including the bis(iminoacyl) $(CO)_3$(CN-xylyl)Mn[C(=N-xylyl)C(=N-xylyl)$CH_2C_6H_4$-*p*-Cl], **3**, and the first octahedrally based tris(iminoacyl) $(CO)_4$Mn[C(=N-xylyl)C(=N-xylyl)C(=N-xylyl)-$CH_2C_6H_4$-*p*-Cl], **6**. The same reaction in THF afforded the carbonyl insertion product $(CO)_3$-(xylyl-NC)$_2$MnC(O)$CH_2C_6H_4$-*p*-Cl, **9**. Reaction of **1** with 1 equiv of xylyl isocyanide in THF without PdO produced the expected acyl $(CO)_4$(CN-xylyl)MnC(O)$CH_2C_6H_4$-*p*-Cl, **11**, along with a minor quantity of **3**. Exposure of the reaction mixture to CO_2 afforded the unique dimanganese species $(CO)_4$Mn[C{=CH(C_6H_4-*p*-Cl)}N-(xylyl)C(O)OMn$(CO)_4$[C(=NH-xylyl)-$CH_2C_6H_4$-*p*-Cl]], **12**, in which the manganese centers are linked through a carbamato bridge. X-ray structures of **3**, **6**, and **12** are reported.

1. Introduction

Organometallic insertion reactions can create new C−C bonds and hence have attracted widespread interest.[2,3] Carbon monoxide insertion has been extensively studied,[4] while insertion reactions of other small molecules are now receiving increasing attention. One class of molecules that has shown insertion chemistry is the isocyanides, CNR.[5] Carbon monoxide and isocyanides are isolobal; therefore, similar types of reactivity are expected for each. Isocyanides are generally regarded as better σ donors and weaker π acceptors than carbon monoxide.[6] Unlike carbon monoxide, isocyanides contain an R group, which can be varied to change the electronic or steric properties.

Molecules containing both CO and CNR ligands often display a competition between CO insertion (giving acyl products) and isocyanide insertion (giving iminoacyl products). The facility of insertion reactions in an Fe system containing both carbonyls and isocyanides was shown to vary in the following order: aromatic isocyanide > CO > aliphatic isocyanide.[7] However, predicting whether acyls or iminoacyls will be formed is not always straightforward. Extended Hückel MO studies suggest that iminoacyls are more thermodynamically stable than their acyl counterparts. Also, the kinetic activation energy barrier is larger for isocyanide insertions.[8] These findings suggest that the transformation of an acyl to the more thermodynamically stable iminoacyl product should be possible. Pizzano and co-workers have now observed the first example of thermal conversion from a molybdenum acyl to a molybdenum iminoacyl complex.[9]

Workers in our laboratory have previously investigated the reaction of alkylpentacarbonylmanganese compounds with various isocyanides.[10−12] Stirring any of several aromatic or aliphatic isocyanides with various benzylpentacarbonylmanganese complexes in THF produces primarily manganese acyls, *p*-$XC_6H_4CH_2C(O)Mn(CNR)(CO)_4$ (X = H, Cl, or OMe), which are the result of carbonylation and isocyanide addition. When the manganese acyls that contain a terminal aliphatic isocyanide are heated, the decarbonylation product, *p*-$XC_6H_4CH_2Mn(CNR)(CO)_4$, results.[12] However, if the isocyanide is aromatic *p*-tolyl isocyanide, thermolysis

* To whom correspondence should be addressed.

(1) (a) University of Cincinnati, Cincinnati, OH. (b) Molecular Simulations Inc., San Diego, CA. (c) The Procter and Gamble Co., Miami Valley Laboratories, Cincinnati, OH.

(2) Collman, J. P.; Hegedus, L. S.; Norton, J. R.; Finke, R. G. *Principles and Applications of Organotransition Metal Chemistry;* University Science Books: Mill Valley, CA, 1987.

(3) Alexander, J. J. In *The Chemistry of the Metal−Carbon Bond, vol.2*; Hartley, F. R., Patai, S., Eds.; J. F. Wiley and Sons: Ltd., London, 1985; p 339.

(4) (a) Wojcicki, A. A. *Adv. Organomet. Chem.* **1973**, *11*, 87. (b) Kuhlmann, E. J.; Alexander, J. J. *Coord. Chem. Rev.* **1980**, *33*, 195.

(5) (a) Singleton, E.; Oosthuizen, H. E. *Adv. Organomet. Chem.* **1983**, *22*, 209. (b) Yamamoto, Y. *Coord. Chem. Rev.* **1980**, *32*, 193. (c) Treichel, P. M. *Adv. Organomet. Chem.* **1973**, *11*, 21.

(6) Cotton, F. A.; Wilkinson, G.; Murillo, C. A.; Bochmann, M. *Advanced Inorganic Chemistry,* 6th ed.; John Wiley & Sons: New York, 1999; p 246.

(7) de Lange, P. P. M.; Fruhauf, H. W.; Kraakman, M. J. A.; van Wijnkoop, M.; Kranenburg, M.; Groot, A. H. J. P.; Vrieze, K.; Fraanje, J.; Wang, Y.; Numan, M. *Organometallics* **1993**, *12*, 417.

(8) Berke, H.; Hoffmann, R. *J. Am. Chem. Soc.* **1978**, *100*, 7724.

(9) Pizzano, A.; Sanchez, L.; Altmann, M.; Monge, A.; Ruiz, C.; Carmona, E. *J. Am. Chem. Soc.* **1995**, *117*, 1759.

(10) Motz, P. L.; Alexander, J. J.; Ho, D. M. *Organometallics* **1989**, *8*, 2589.

(11) Motz, P. L.; Williams, J. P.; Alexander, J. J.; Ho, D. M. *Organometallics* **1989**, *8*, 1523.

(12) Kuty, D. W.; Alexander, J. J. *Inorg. Chem.* **1978**, *17*, 1489.

10.1021/om9903644 CCC: $18.00
Publication on Web 12/02/1999

yields a diazabutadiene dimer, **A**.[11] The proposed mechanism suggests formation of a highly reactive (alkyl)(isocyanide) intermediate resulting from decarbonylation followed by rapid and preferential insertion of aromatic isocyanide to give a Mn iminoacyl intermediate, which dimerizes.

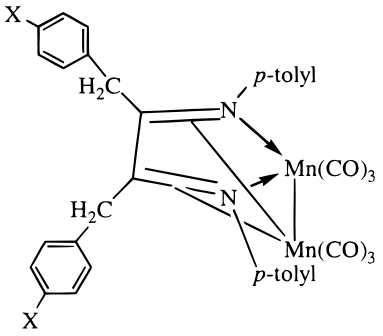

A (X = Cl, H, OMe)

Reactions of benzyl manganese carbonyls with *p*-tolyl isocyanide in the presence of PdO were studied in order to isolate simple isocyanide substitution products rather than carbonylation products.[10] PdO has been shown to catalyze the substitution of CO by isocyanides.[13−15] The anticipated products were $(CNR)(CO)_4MnCH_2C_6H_4$-*p*-X, containing a terminal *p*-tolyl isocyanide. However, when the reaction was run in toluene with PdO, only isocyanide insertion products were isolated.

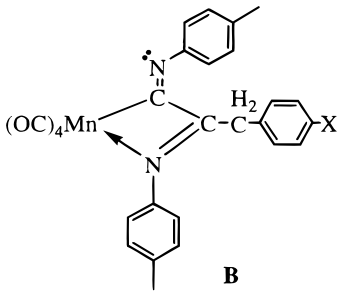

B

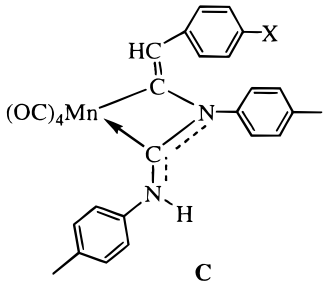

C

Complexes **B** and **C**, which contain 2 equiv of isocyanide, were isolated even if the reagents were mixed in a 1:1 ratio. It has been shown that **C** is the kinetic product that converts to the thermodynamic product, **B**, over time.[11,16]

The reaction of manganese alkyls with *p*-tolyl isocyanide, with and without PdO, results in products containing inserted isocyanides (**A**, **B**, **C**). It is of interest to attempt to isolate intermediates in these reactions in order to gain more information on the mechanism of their production. Previous work in this laboratory suggests that insertion of *p*-tolyl isocyanide in manganese alkyl species is rapid.[10,11] However, a study of rhenium complexes in acetonitrile showed that the insertion of the bulky aromatic 2,6-dimethylphenyl isocyanide (xylyl isocyanide) is significantly slower than that of *p*-tolyl isocyanide. The rate of insertion of xylyl isocyanide into rhenium−carbon bonds was found to be slower than *p*-tolyl isocyanide by approximately a factor of 2.[17] Yamamoto and co-workers[18] and de Lange and co-workers[7] have estimated the relative sizes of isocyanide ligands. de Lange developed cone angles in a manner similar to the development for phosphines.[19] The slower insertion of the larger xylyl group (remote cone angle = 69°) in the Re system[17] compared with *p*-tolyl (remote cone angle measured for phenyl isocyanide = 57°) indicates that the size of the aromatic isocyanide is important in its insertion chemistry on Re. These results prompted us to investigate the reactions of alkylpentacarbonylmanganese complexes with xylyl isocyanide and to compare the results to those obtained with aliphatic isocyanides and the smaller aromatic isocyanide, *p*-tolyl isocyanide.

2. Results and Discussion

2.1. Reaction in Toluene in the Presence of PdO. Reactions of $(CO)_5MnCH_2C_6H_4$-*p*-Cl (**1**) with 2 equiv of xylyl isocyanide in the presence of PdO in toluene at room temperature were investigated under conditions similar to those of the *p*-tolyl isocyanide investigation.[11] Multiple products were isolated from the reaction mixture. One minor product, $Mn_2(CO)_9$(xylyl-NC) (**2**), is isolated in approximately a 7% yield. It is the result of the reduction of **1**. Reduction of manganese(I) carbonyl complexes by an aromatic isocyanide to afford substitution products of dimanganese decacarbonyls has been reported by Joshi and co-workers.[20] Also, small amounts of $Mn_2(CO)_8$(CN-*p*-tolyl)$_2$ and $Mn_2(CO)_9$(CN-*p*-tolyl) were isolated by Motz[21] from the reaction of **1** with *p*-tolyl isocyanide in THF at room temperature. Complex **2** has previously been reported by Albers and Coville, and the spectroscopic data for **2** match those in the literature.[13]

All other products (**3**, **4**, **5**, and **6**) isolated from the reaction are depicted in Scheme 1 and are the result of multiple isocyanide insertions. The product isolated in the highest yield from the PdO-catalyzed reaction is a manganese bis(iminoacyl) metallacycle, **3**. The manganese complex, **3**, is a tricarbonyl species containing a terminal xylyl isocyanide and a manganacycle that is the result of insertion of 2 equiv of xylyl isocyanide into the metal−alkyl bond. It is similar to the *p*-tolyl manganacycle **B** with the following exceptions: xylyl isocyanides replace *p*-tolyl isocyanides, and a terminal

(13) Albers, M. O.; Coville, N. J. *S. Afr. J. Chem.* **1982**, *35*, 139.
(14) Harris, G. W.; Coville, N. J. *Organometallics* **1985**, *4*, 908.
(15) Coville, N. J.; Stolzenberg, A. M.; Muetterties, E. L. *J. Am. Chem. Soc.* **1983**, *105*, 2499.
(16) Laughlin, S. K.; Alexander, J. J. Unpublished results.
(17) Padolik, L. L.; Alexander, J. J.; Ho, D. M. *J. Organomet. Chem.* **1992**, *440*, 153.
(18) Yamamoto, Y.; Aoki, K.; Yamazaki, H. *Inorg. Chem.* **1979**, *18*, 1681.
(19) Tolman, C. A. *J. Am. Chem. Soc.* **1970**, *92*, 2956.
(20) Joshi, K. K.; Pauson, P. L.; Stubbs, W. H. *J. Organomet. Chem.* **1963**, *1*, 51.
(21) Motz, P. L. Ph.D. Dissertation, University of Cincinnati, 1988, p 107.

Scheme 1

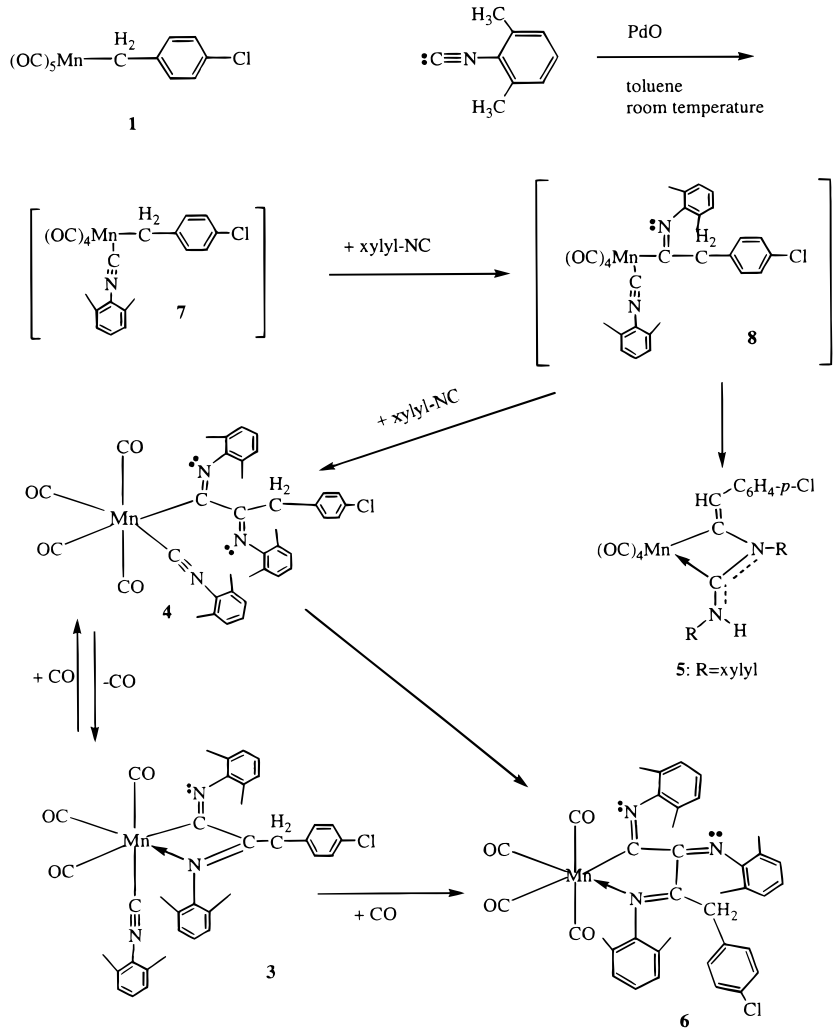

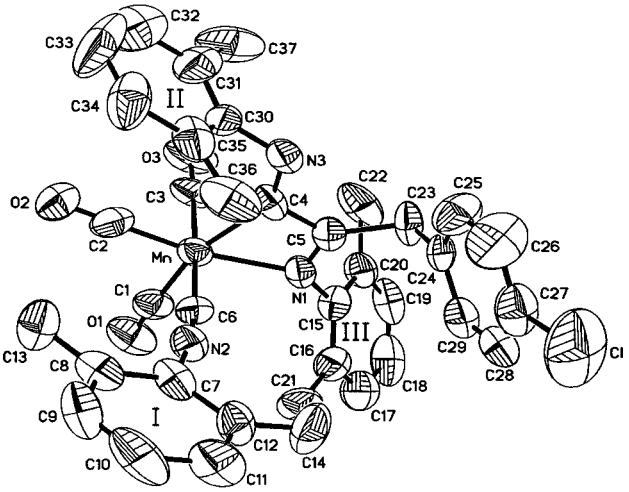

Figure 1. ORTEP diagram of **3**.

xylyl isocyanide replaces a terminal CO, giving a *fac*-tricarbonyl product. Interestingly, the xylyl isocyanide tetracarbonyl product analogous to **B** was not isolated.

The structure of **3** has been confirmed by single-crystal X-ray analysis. An ORTEP diagram of **3** is shown in Figure 1. Crystal and diffraction data, including bond angles and distances, are listed in Tables 1 and 2. Complex **3** contains a four-membered bis(iminoacyl) ring composed of Mn, N1, C5, and C4. The geometry around Mn is a distorted octahedron. The bite of the bis-(iminoacyl) is 64.4 (4)°. The three carbonyls are essentially linear, and the terminal isocyanide angle, ∠Mn−C(6)−N(2), is 173.6 (11)°. The C(5)−N(1)−C(15) angle and the C(4)−N(3)−C(30) angle around the sp^2 nitrogens are 126.1(10)° and 118.8(10)°, respectively.

The N(1)−C(5) and C(4)−N(3) bond distances of 1.300(13) and 1.275(13) Å, respectively, are as expected for C−N double bonds. The Mn−C(4) distance of 2.039-(12) Å is rather short for a manganese−acyl bond[22] but only slightly shorter than the Mn−iminoacyl bond distance of 2.067 Å in **B**.[10] The Mn−N(1) distance of 2.115(9) Å is slightly longer that the Mn−imine N distance of 2.079 Å in **B**[10] and in a similar bis-(iminoacyl), four-membered manganacycle reported by Cooper and co-workers.[23] The terminal CO distances are typical of those in alkyl manganese carbonyl complexes.[22] The Mn−C(6) bond length of the terminal isocyanide is 1.945(13) Å and the C−N triple bond distance is 1.137(13) Å, which are usual for manganese isocyanide complexes.[24]

The IR, ^{13}C NMR, and mass spectra are consistent with the structure shown and are unremarkable. The

(22) Treichel, P. M. In *Comprehensive Organometallic Chemistry, vol. 4*; Wilkinson, G., Stone, F. G. A., Abel, E. W., Eds.; Pergamon Press: New York, 1982; pp 1−159.

(23) Utz, T. L.; Leach, P. A.; Gieb, S. J.; Cooper, N. J. *Organometallics* **1997**, *16*, 4109.

Table 1. Summary of Crystal Data for 3, 6, and 12

Crystal Data and Structure Refinement for **3**	
empirical formula	$C_{37}H_{33}ClMnN_3O_3$
fw	658.05
temp	294(2) K
wavelength	1.54178 Å
cryst syst	orthorhombic
space group	*Pbca*
unit cell dimens	$a = 18.239(6)$ Å; $\alpha = 90°$ $b = 15.971(5)$ Å; $\beta = 90°$ $c = 23.062(7)$ Å; $\gamma = 90°$
volume, *Z*	6718(4) Å^3, 8
density (cald)	1.301 Mg/m^3
abs coeff	4.242 mm^{-1}
F(000)	2736
cryst size	0.20 × 0.20 × 0.10 mm
θ range for data collection	3.83−60.02°
limiting indices	$0 < h < 20$, $0 < k < 17$, $0 < l < 25$
no. of reflns collected	5183
no. of indep reflns	4988
refinement method	full-matrix least-squares on F^2
no. of data/restraints/params	4976/0/407
goodness-of-fit on F^2	1.028
final *R* indices [$I > 2\sigma(I)$]	R1 = 0.0882, wR2 = 0.1925
R indices (all data)	R1 = 0.2871, wR2 = 0.2975
extinction coeff	0.00042(7)
largest diff peak and hole	0.350 and −0.616 e Å^{-3}
Crystal Data and Structure Refinement for **6**	
empirical formula	$C_{38}H_{33}ClMnN_3O_4$
fw	686.06
temp	296(2) K
wavelength	0.71073 Å
cryst syst	monoclinic
space group	$P2_1/n$
unit cell dimens	$a = 10.317(1)$ Å; $\alpha = 90°$ $b = 19.602(1)$ Å; $\beta = 99.89(1)°$ $c = 17.113(1)$ Å; $\gamma = 90°$
volume, *Z*	3409.4(3) Å^3, 4
density (calcd)	1.337 Mg/m^3
abs coeff	0.510 mm^{-1}
F(000)	1424
cryst size	0.50 × 0.25 × 0.10 mm
θ range for data collection	1.59−28.31°
limiting indices	$-13 < h < 11$, $-21 < k < 25$, $-12 < l < 22$
no. of reflns collected	16370
no. of indep reflns	7947 ($R_{int} = 0.0505$)
refinement method	full-matrix least-squares on F^2
no. of data/restraints/params	6869/0/424
goodness-of-fit on F^2	1.035
final *R* indices [$I > 2\sigma(I)$]	R1 = 0.0543, wR2 = 0.0930
R indices (all data)	R1 = 0.1463, wR2 = 0.1269
largest diff peak and hole	0.254 and −0.233 e Å^{-3}
Crystal Data and Structure Refinement **12**	
empirical formula	$C_{41}H_{30}Cl_2Mn_2N_2O_{10}$
fw	891.45
temp	296(2) K
wavelength	1.54184 Å
cryst syst	triclinic
space group	$P\bar{1}$
unit cell dimens	$a = 11.841(2)$ Å; $\alpha = 97.18(3)°$ $b = 12.160(2)$ Å; $\beta = 105.32(3)°$ $c = 15.940(3)$ Å; $\gamma = 98.40(3)°$
volume, *Z*	2157.4(7) Å^3, 2
density (calcd)	1.372 Mg/m^3
abs coeff	6.375 mm^{-1}
F(000)	908
cryst size	0.25 × 0.20 × 0.15 mm
θ range for data collection	2.0−58.0°
limiting indices	$0 < h < 12$, $-13 < k < 13$, $-17 < l < 16$
no. of reflns collected	6421
no. of indep reflns	5881 ($R_{int} = 0.0165$)
refinement method	full-matrix least-squares on F^2
no. of data/restraints/params	5881/0/518
goodness-of-fit on F^2	0.961
final *R* indices [$I > 2\sigma(I)$]	R1 = 0.0656, wR2 = 0.1376
R indices (all data)	R1 = 0.1226, wR2 = 0.1619
extinction coeff	0.00042(11)
largest diff peak and hole	0.314 and −0.250 e Å^{-3}

Table 2. Selected Bond Distances [Å] and Angles [deg] for 3

Mn−C(2)	1.78(2)	Mn−C(3)	1.808(11)
Mn−C(1)	1.825(14)	Mn−C(6)	1.945(12)
Mn−C(4)	2.039(11)	Mn−N(1)	2.120(9)
Mn−C(5)	2.587(12)	O(1)−C(1)	1.146(13)
O(2)−C(2)	1.142(13)	O(3)−C(3)	1.152(11)
N(1)−C(5)	1.300(13)	N(2)−C(6)	1.137(13)
N(2)−C(7)	1.416(14)	N(3)−C(4)	1.275(13)
N(3)−C(30)	1.419(14)	C(4)−C(5)	1.47(2)
C(5)−C(23)	1.523(14)		
C(2)−Mn−C(3)	88.5(6)	C(2)−Mn−C(1)	93.8(6)
C(3)−Mn−C(1)	91.5(5)	C(2)−Mn−C(6)	86.1(5)
C(3)−Mn−C(6)	171.3(5)	C(1)−Mn−C(6)	95.7(5)
C(2)−Mn−C(4)	102.7(6)	C(3)−Mn−C(4)	89.6(5)
C(1)−Mn−C(4)	163.5(6)	C(6)−Mn−C(4)	85.0(5)
C(2)−Mn−N(1)	167.1(5)	C(3)−Mn−N(1)	91.0(5)
C(1)−Mn−N(1)	99.1(5)	C(6)−Mn−N(1)	92.8(4)
C(4)−Mn−N(1)	64.4(4)	C(2)−Mn−C(5)	137.1(5)
C(3)−Mn−C(5)	90.9(5)	C(1)−Mn−C(5)	129.1(5)
C(6)−Mn−C(5)	88.4(4)	C(4)−Mn−C(5)	34.4(4)
N(1)−Mn−C(5)	30.0(3)	C(5)−N(1)−C(15)	126.1(10)
C(5)−N(1)−Mn	95.3(7)	C(15)−N(1)−Mn	137.8(7)
C(6)−N(2)−C(7)	171.2(13)	C(4)−N(3)−C(30)	118.8(10)
O(1)−C(1)−Mn	176.2(12)	O(2)−C(2)−Mn	179.1(13)
O(3)−C(3)−Mn	177.2(13)	N(3)−C(4)−C(5)	119.4(10)
N(3)−C(4)−Mn	146.8(10)	C(5)−C(4)−Mn	93.7(8)
N(1)−C(5)−C(4)	106.5(10)	N(1)−C(5)−C(23)	126.2(11)
C(4)−C(5)−C(23)	127.3(11)	N(1)−C(5)−Mn	54.7(6)
C(4)−C(5)−Mn	51.9(6)	C(23)−C(5)−Mn	178.6(8)
N(2)−C(6)−Mn	173.6(11)		

room-temperature ^{1}H NMR spectrum of **3** contains a multiplet from 7.21 to 6.92 ppm due to the phenyl protons. An AB quartet is observed at 3.59 ppm (J = 12.25 Hz) due to the diastereotopic methylene protons. The methyl region contains three sharp signals at 2.25, 2.18, and 2.07 ppm. Very broad peaks are also evident between 2.40 and 2.10 ppm. The broadening suggests that a dynamic process is occurring involving some of the xylyl methyl groups at room temperature, vide infra.

Complex **3** contains three xylyl isocyanides. One is in a terminal position on the metal, contains C(6) (from the crystal structure solution), and is labeled **I** in Figure 1. The other two xylyl groups are labeled as **II** and **III**. Xylyl **II** is part of the iminoacyl group in which the carbon is labeled as C(4) and the nitrogen is not directly included in the metallacycle. Xylyl **III** is part of the iminoacyl in which both the carbon C(5) and the nitrogen N(1) are incorporated into the manganacycle.

Variable-temperature ^{1}H NMR gives some insight into the dynamic process that these xylyl groups undergo and the assignments of their methyl groups. Figure 2 shows the ^{1}H NMR methyl region at various temperatures. At various temperatures overlap of signals occurs; however the −30 °C spectrum begins to show all five resonances that are resolved at lower temperatures. The −30 °C spectrum contains signals at 2.37, 2.27, 2.14, 2.13, and 2.06 ppm. There is some overlap of the 2.14 and 2.13 peaks. The integration of these peaks is 1:1:2:1:1, respectively, which is appropriate for six methyl groups. As the temperature increases, two peaks (formerly located at 2.37 and 2.13 ppm) broaden until coalescence occurs at approximately 30 °C. The exact coalescence temperature is difficult to

(24) (a) Bright, D.; Mills, O. S. *J. Chem. Soc.* **1974**, 219. (b) Sarapu, A. C.; Fenske, R. F. *Inorg. Chem.* **1972**, *11*, 3021. (c) Ericsson, M.-S.; Jagner, S.; Ljungström, E. *Acta Chem. Scand., Ser. A* **1980**, *A34*, 535. (d) Ericsson, M.-S.; Jagner, S.; Ljungström, E. *Acta Chem. Scand., Ser. A* **1979**, *A33*, 371.

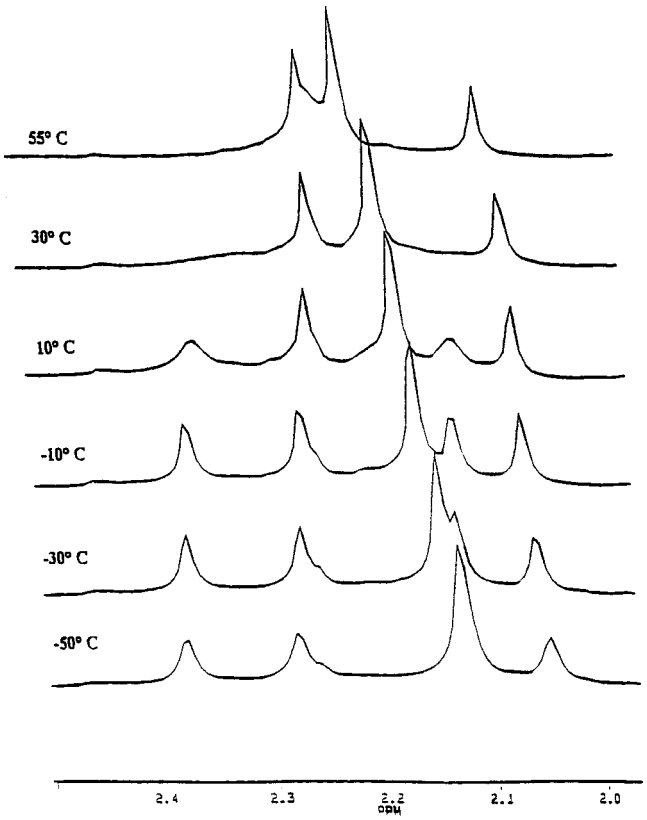

Figure 2. Variable-temperature ^{1}H NMR for **3**.

determine due to the overlap of other methyl signals complicating the spectrum. A new peak begins to form at 2.24 ppm in the 55 °C spectrum. A $\Delta G^{\ddagger}$ of 61.5 kJ/mol for the dynamic process leading to the methyl exchange was calculated on the basis of the Eyring equation.[25] The rate constant used in the calculation of $\Delta G^{\ddagger}$ was approximated from the change in the line widths of an NMR peak in the slow exchange region (−50 to 20 °C). The other three peaks remain essentially unchanged. There are slight shifts in some of the peaks of the nonexchanging methyls in the ^{1}H NMR due to the overlap with the dynamic signals.

These results indicate that there are three distinct xylyl groups. One exhibits fast exchange on the NMR time scale at all temperatures. This gives rise to the signal at 2.14 ppm at −30 °C. In another xylyl group, methyl exchange does not occur to any significant extent; this group gives rise to two distinct methyl signals at all temperatures (2.27 and 2.06 ppm at −30 °C). The third xylyl group exhibits slow exchange at lower temperatures and increasingly rapid exchange by rotation at higher temperatures (2.37 and 2.13 ppm at −30 °C and 2.24 ppm at 55 °C). The exchange mechanism is presumably rotation around the N−C(ipso) bond.

To determine which xylyl groups in **3** exhibit fast rotation, no rotation, and rotation of varying frequency, molecular dynamics simulations were performed at several temperatures (see Experimental Section for simulation details). Solvent considerations were not taken into account in the molecular simulations. The temperatures for the dynamics studies should be considered as relative but not absolute. The total time interval studied in each simulation was 50 ps. The simulation found the torsion angle of xylyl **I** (defined as C4−Mn−C7−C12) varies at all temperatures, indicating rapid rotation. The torsion angle of xylyl **II** (C4−N3−C30−C35) is essentially fixed at low temperatures, and rotation frequency increases as the temperature increases. The simulation at various temperatures suggests the torsion angle of xylyl **III** (Mn−N1−C15−C16) over time does not change, suggesting that xylyl **III** does not rotate even at higher temperatures.

The dynamics simulation agrees with the observed variable-temperature ^{1}H NMR signals from the methyl groups on the xylyl isocyanide and assists in their assignments. The freely rotating group, xylyl **I**, is on the terminal isocyanide and corresponds to the room-temperature ^{1}H NMR signal at 2.18 ppm. The other two xylyl ligands are incorporated into the manganacycle. Xylyl **II** is the group in which the iminoacyl carbon is found in the four-membered metallacycle and the nitrogen is not located in the ring. The frequency of rotation of xylyl **II** increases as the temperature increases and therefore fits the observed room-temperature ^{1}H NMR broad peak at 2.24 ppm. Both the carbon and the nitrogen of xylyl **III** are located in the ring of the metallacycle. Xylyl **III** has essentially no rotation at tested temperatures and corresponds to the room-temperature ^{1}H NMR signals at 2.25 and 2.07 ppm. These results indicate that the manganacycle restricts the rotation of the included xylyl groups.

Another bis(iminoacyl) complex, **4**, is isolated in trace amounts from the PdO-catalyzed reaction in toluene. The spectroscopic data are consistent with the proposed structure, which contains a "dangling" bis(iminoacyl) group. A complex similar to **4** was isolated by Motz[10] and co-workers. They isolated a manganese tetracarbonyl with a bulky terminal *tert*-butyl isocyanide and a "dangling" bis(iminoacyl) ligand formed from *p*-tolyl isocyanides. The spectroscopic data for each "dangling" bis(iminoacyl) are similar.

The ^{1}H NMR spectrum of **4** contains a multiplet due to aromatic protons, a singlet at 3.51 ppm from the benzylic protons, and singlets at 2.31, 2.11, and 2.01 ppm from the xylyl methyl groups. Unlike **3**, all methyl signals of **4** are sharp at room temperature, suggesting free rotation around the N−C bonds. Also unlike the ^{1}H NMR of **3**, the benzylic protons in the ^{1}H NMR of **4** give rise to a singlet. This is consistent with the existence of a plane of symmetry in **4** containing the metal, two carbonyls, the terminal isocyanide, and the dangling ligand coupled with free rotation around the C−C and C−N bonds; thus, the methylene protons are equivalent by NMR.

Another product, isolated as a colorless solid, is the cyclic carbene **5**, the xylyl isocyanide analogue of **C** that was isolated by Motz and co-workers.[10] The spectral data of **5** compare favorably with data previously reported for **C**. Some features include an N−H signal in the IR spectrum at 3296 cm^{-1}, a broad peak at 7.04 ppm in the ^{1}H NMR spectrum arising from N−H, and a peak at 6.40 ppm from the olefinic proton.

Also isolated from the reaction is the green solid **6**. The green color is in stark contrast to the other Mn(I) species containing isocyanide and/or iminoacyl ligands,

(25) Günther, H. *NMR Spectroscopy*, 2nd ed.; John Wiley and Sons: Chichester, England, 1995; p 342.

Table 3. Selected Bond Distances [Å] and Angles [deg] for 6

Mn−C(1)	1.819(4)	Mn−C(4)	1.831(4)
Mn−C(3)	1.844(4)	Mn−C(2)	1.860(4)
Mn−C(5)	2.067(3)	Mn−N(1)	2.082(2)
O(1)−C(1)	1.144(3)	O(2)−C(2)	1.134(4)
O(3)−C(3)	1.144(3)	O(4)−C(4)	1.145(4)
N(1)−C(7)	1.293(4)	N(1)−C(31)	1.461(4)
N(2)−C(5)	1.274(4)	N(3)−C(6)	1.273(4)
C(5)−C(6)	1.519(4)	C(6)−C(7)	1.491(4)
C(7)−C(24)	1.505(4)		
C(1)−Mn−C(4)	89.2(2)	C(1)−Mn−C(3)	89.58(14)
C(4)−Mn−C(3)	94.41(14)	C(1)−Mn−C(2)	86.6(2)
C(4)−Mn−C(2)	170.43(14)	C(3)−Mn−C(2)	94.1(2)
C(1)−Mn−C(5)	98.68(13)	C(4)−Mn−C(5)	84.34(13)
C(3)−Mn−C(5)	171.62(13)	C(2)−Mn−C(5)	87.84(13)
C(1)−Mn−N(1)	178.86(12)	C(4)−Mn−N(1)	90.88(12)
C(3)−Mn−N(1)	91.55(12)	C(2)−Mn−N(1)	93.21(12)
C(5)−Mn−N(1)	80.19(11)	C(7)−N(1)−C(31)	120.3(3)
C(7)−N(1)−Mn	119.0(2)	C(31)−N(1)−Mn	120.7(2)
O(1)−C(1)−Mn	175.5(3)	O(2)−C(2)−Mn	175.8(3)
O(3)−C(3)−Mn	177.2(3)	O(4)−C(4)−Mn	177.3(3)
N(2)−C(5)−C(6)	113.5(3)	N(2)−C(5)−Mn	136.6(2)
C(6)−C(5)−Mn	109.8(2)	N(3)−C(6)−C(7)	115.7(3)
N(3)−C(6)−C(5)	129.9(3)	C(7)−C(6)−C(5)	114.2(3)
N(1)−C(7)−C(6)	114.3(3)	N(1)−C(7)−C(24)	125.2(3)
C(6)−C(7)−C(24)	120.6(3)		

which are generally yellow, red, or colorless. The green color is likely a result of increased conjugation within the complex. The spectral data are consistent with the tris(iminoacyl) complex pictured in Scheme 1. This is, to our knowledge, the first isolated octahedrally based tris(iminoacyl) complex. The IR has four strong bands between 2068 and 1954 cm^{-1}, consistent with a tetracarbonyl complex. The ^1H NMR indicates aromatic, methylene, and methyl protons in the expected regions with proper ratios.

From the spectroscopic data it is unclear whether **6** is a five-membered metallacycle (a possible resultant from ring closure by the imino nitrogen of the first inserted isocyanide) or a four-membered metallacycle (a possible resultant from ring closure by the imino nitrogen of the second inserted isocyanide). Previous work suggested that the probable structure was **6**. First, the square-planar Pd and Ni tris(iminoacyl) complexes exhibited a structure that contains five atoms in the metallacycle.[26−28] Second, manganese five-membered rings are less constrained than four-membered rings in pseudo-octahedral complexes, allowing for an N−Mn−C angle closer to the 90°.

A single-crystal X-ray structure solution was performed to confirm the structure of **6**. Crystallographic parameters can be found in Table 1, and selected bond angles and distances are recorded in Table 3. An ORTEP diagram of **6** is shown as Figure 3. This pseudo-octahedral complex has an angle of 84.34(13)° for C4−Mn−C5, which is slightly larger than those found in five-membered bis(iminoacyl) metallacycles of palladium and nickel (80.3−81.3°).[26−28] All other angles and distances are unremarkable.

The mixture produced from the reaction depicted in Scheme 1 in toluene contains products **2**−**6**. The dimer

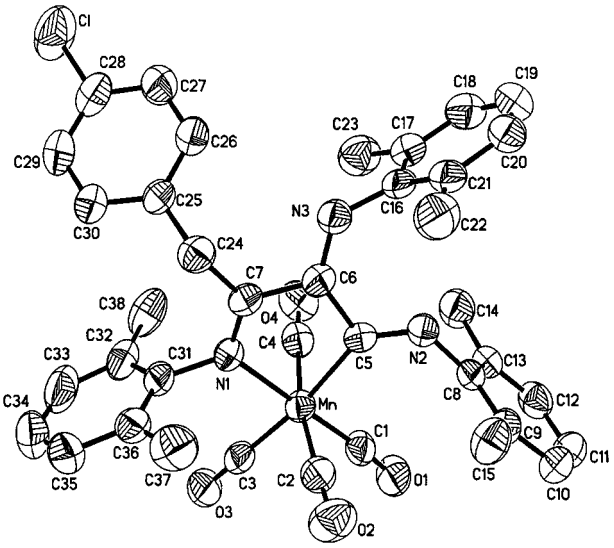

Figure 3. ORTEP diagram of **6**.

2 is produced from the reduction of the starting material by added isocyanide, as discussed earlier. The proposed mechanism for the formation of the isocyanide insertion products **3**−**6** is shown in Scheme 1.

The initial step is likely the PdO-catalyzed substitution of a carbonyl by an isocyanide to create intermediate **7**, which is neither isolable nor spectroscopically observable. Rapid migration of the benzyl group to the isocyanide carbon and addition of a second equivalent of xylyl isocyanide leads to the mono(iminoacyl) intermediate **8** (which also is neither observed nor isolated). From this intermediate, two pathways are possible. Product **5** is formed by attack on the polarized terminal isocyanide carbon by the imino nitrogen lone pair followed by migration of a proton from the benzyl carbon to the isocyanide nitrogen. This pathway to a cyclic carbene is also proposed in the *p*-tolyl isocyanide chemistry previously reported.[10] If intermediate **8** inserts the second added isocyanide and the vacant coordination site is taken by a third isocyanide, the "dangling" bis(iminoacyl) **4** is produced. Then, a third isocyanide insertion followed by ring closure by the imino nitrogen lone pair leads to the green solid **6**. If a terminal carbonyl is displaced in **4** by the ring closure from the imino nitrogen coordination to the manganese, manganacycle **3** is created. Other studies within our group indicate that **3** converts to **6** stirring under a CO atmosphere.[29]

The observed reactivity and proposed mechanism with xylyl isocyanide are similar in some aspects to the chemistry found with *p*-tolyl isocyanide (earlier described in the Introduction), although different in significant other aspects.[10] Both aromatic isocyanides form cyclic carbenes (**5** and **C**) from their reactions with **1**. The *p*-tolyl cyclic carbene **C** rearranges to the tetracarbonyl bis(iminoacyl)metallacycle **B**. However the xylyl cyclic carbene **5** does not undergo this transformation and is stable over 7 days at 50 °C in $CDCl_3$. The reason for this is unclear.

The major product from the *p*-tolyl reaction is the tetracarbonyl bis(iminoacyl) **B**. The xylyl isocyanide analogue of **B** is not observed. Instead, three other

(26) Yamamoto, Y.; Tanase, T.; Yanai, T.; Asano, T.; Kobayashi, K. *J. Organomet. Chem*. **1993**, *456*, 287.
(27) Carmona, E.; Marín, J. M.; Palma, P.; Poreda, M. L. *J. Organomet. Chem*. **1989**, 377, 157.
(28) Tanase, T.; Ohizumi, T.; Kobayashi, K.; Yamamoto, Y. *Organometallics* **1996**, *15*, 3404.
(29) Homrighausen, C. L.; Alexander J. J. Unpublished results.

Scheme 2

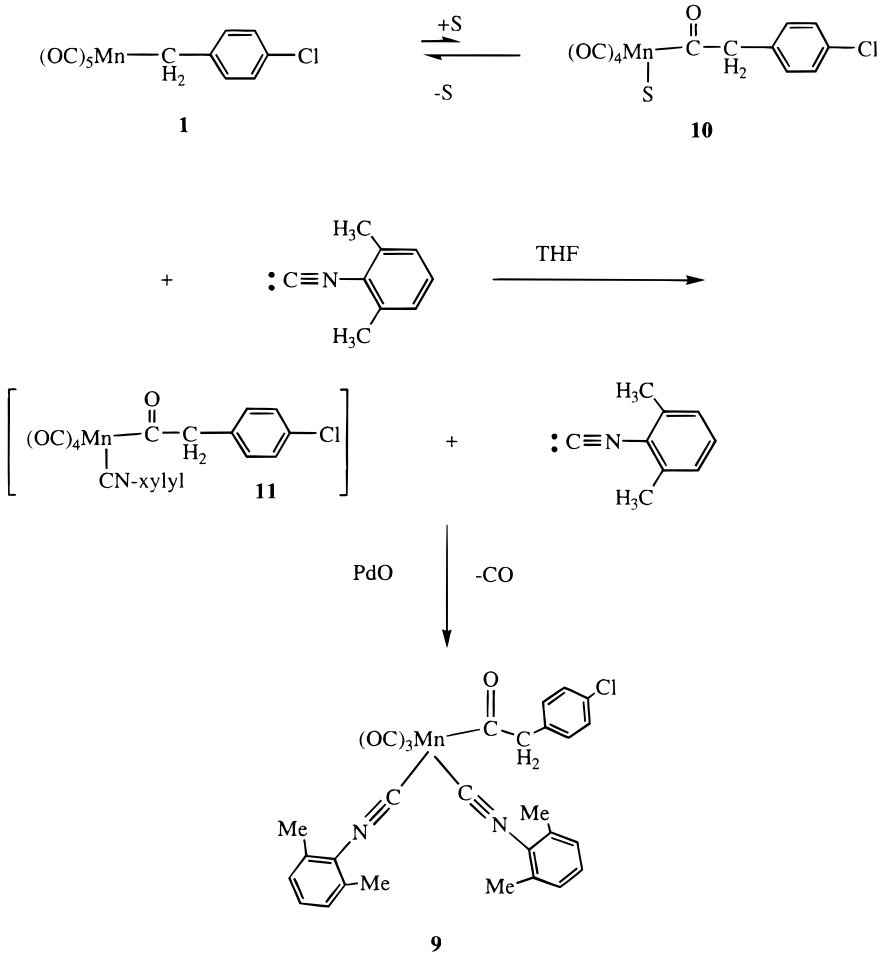

products are isolated: **3**, **4**, and **6**. The proposed mechanisms of the reaction of **1** with *p*-tolyl and xylyl isocyanide both include an intermediate, which contains one inserted isocyanide and one terminal isocyanide (**8** in Scheme 1). *p*-Tolyl isocyanide undergoes a second insertion followed by rapid coordination of the imino nitrogen to the manganese to form the tetracarbonyl manganacycle **B**. Xylyl isocyanide also undergoes an insertion of a second isocyanide; however, instead of coordination of the imino nitrogen to the vacant coordination site on the metal, a third equivalent of xylyl isocyanide fills the vacant manganese site to produce **4**. Apparently, the bulk of the xylyl isocyanide slows the attack by the imino nitrogen on the metal and, instead, the coordination of a free isocyanide is favored. If a carbonyl in **4** is displaced by ring closure, then the metallacycle **3** is formed. Alternatively, **4** can insert a third isocyanide followed by ring closure to form the tris(iminoacyl) manganacycle **6**. Surprisingly, this third insertion is found only with the larger xylyl isocyanide. A third insertion of isocyanide is favored for xylyl isocyanide presumably because coordination of a third equivalent of isocyanide is faster than ring closure which forms bis(iminoacyl) metallacycles.

2.2. Reaction in THF in the Presence of PdO. The same reaction performed in THF (Scheme 2) affords different products. The only product identified and isolated from the THF reaction is the disubstituted acyl $(CO)_3(xylyl\text{-}NC)_2MnC(O)CH_2C_6H_4$-*p*-Cl, **9**, in 29% yield. The IR spectrum of **9** displays two bands at 2161 and 2124 cm^{-1} from the symmetric and antisymmetric C≡N stretches, typical facial tricarbonyl absorptions, and a broad stretch at 1628 cm^{-1} characteristic of a metal acyl. The spectroscopic results are similar to those for the *tert*-butyl isocyanide analogue of **9**.[16]

The proposed mechanism of this reaction is depicted in Scheme 2. The key step that differentiates this reaction from the one in toluene is the equilibrium between **1** and **10**, where S is the coordinating solvent THF. This equilibrium lies much further to the left in toluene. This solvent-dependent equilibrium has been proposed for other carbonylations on manganese and iron.[3] The labile solvent ligand in the acyl **10** is rapidly replaced with xylyl isocyanide, producing **11**. This complex is not isolated because, in the presence of PdO, a carbonyl is rapidly substituted by a second equivalent of isocyanide, producing the stable *fac*-tricarbonyl **9**. It is unlikely that substitution occurs before carbonylation. It has been observed (see Scheme 1) that, if terminal carbonyls and a terminal aromatic isocyanide are present, isocyanide insertion is favored over carbonylation. Hence, if substitution were the first step, iminoacyls (not an acyl) would form. Iminoacyl products might be expected to result from the decarbonylation of **11**. However, no products of this type were observed in this room-temperature reaction.

2.3. Reaction without PdO in THF. Reaction of **1** with xylyl isocyanide in THF (without PdO) was also investigated. As earlier indicated, a number of other

isocyanides react with **1** under these conditions to produce products of carbonylation with the addition of a terminal isocyanide *p*-X-$C_6H_4CH_2C(O)Mn(CO)_4(CNR)$. A 1:1 ratio of xylyl isocyanide and **1** was stirred at room temperature. The IR spectrum and the ^1H NMR spectrum of the reaction mixture both indicate that three complexes are present. One complex isolated from the reaction mixture is unreacted starting material **1**. Another product is the expected manganese tetracarbonyl acyl with a terminal xylyl isocyanide **11**. An additional isolated complex is the bis(iminoacyl) metallacycle **3**, which contains a terminal xylyl isocyanide. By employing a 1:1 ratio of **1**:xylyl isocyanide, one would expect leftover **1** if the metallacycle **3** (which requires 3 equiv of xylyl isocyanide) is produced. The formation of a bis(iminoacyl) manganacycle in this reaction has precedent. Reaction of **1** with *p*-tolyl isocyanide also produces a bis(iminoacyl) minor product.[21] However, **3** is a bis(iminoacyl) tricarbonyl complex with a terminal isocyanide, while the *p*-tolyl bis(iminoacyl) is the tetracarbonyl complex, **C**.

The ratio of species in the reaction mixture was determined by ^1H NMR. The methylene proton peak areas for each complex were determined and their ratios calculated. This integration determined that the product mixture consists of 44% **1**, 34% **11**, and 22% **3**. This ratio of species and the IR spectrum indicate that 100% of the isocyanide has been consumed in the formation of **11** and **3** (1 mol of xylyl-NC in each mole of **11** = 0.34 equiv and 3 mol of xylyl-NC in each mole of **3** = 3 × 0.22 = 0.66 equiv). Although significant amounts of both **11** and **3** are present in the reaction mixture, purification by column chromatography and recrystallization resulted in low isolated yields of pure products **11** and **3** (2% and 11%, respectively). The spectroscopic data are appropriate for complex **11** and are consistent with those of other manganese acyls previously reported.[12]

Other xylyl isocyanide insertion products (such as **6**) apparently are not present in the reaction in THF without PdO (or are present in trace amounts) as they are not resolved from the ^1H NMR baseline of the reaction mixture. In THF, a dissociative CO substitution (via ring closure) is apparently favored to produce the bis(iminoacyl) **3** over the insertion of a third isocyanide to produce the tris(iminoacyl) **6**, which was obtained in toluene. A dissociative mechanism for carbonyl substitution has been previously shown for several Mn(I) complexes.[30] It is reasonable to suggest that in polar THF, the intermediate or transition state for dissociative substitution of CO may be more stable than in toluene, thus affording only **3** in THF. The bulk of the isocyanide may also contribute to a smaller rate for the third insertion than that for ring closure. The barrier seems not to be thermodynamic since **6** is stable in THF solution.

During the workup of the reaction mixture, an unexpected yellow crystalline solid, **12**, was isolated in 6% yield. This product was not in the original reaction mixture and so was formed during the workup, which was not performed under an argon atmosphere. Complex **12** is a manganese dimer with each manganese center containing four terminal carbonyls. The manganese centers are linked through a carbamato bridge. The dimer contains two inserted isocyanides, one on each metal center. A five-membered manganacycle is formed on one metal center. Hydrogen transfer (formally from the benzylic group attached to the metallacycle) to an imino nitrogen has also occurred.

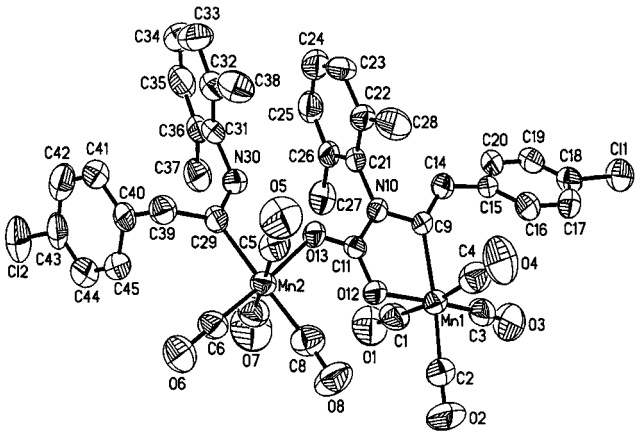

Figure 4. ORTEP diagram of **12**.

The structure of **12** has been established by single-crystal X-ray analysis. An ORTEP diagram of **12** is shown in Figure 4. Crystal and diffraction data are listed in Table 1, and bond angles and distances are listed in Table 4.

Complex **12** contains a five-member metallacycle consisting of Mn(1)−C(9)−N(10)−C(11)−O(12). The mean deviation from this plane is 0.0416 Å; the dihedral angle between this plane and the plane defined by Mn(2)−O(13)−C(8)−C(6)−C(29) is 17°. The coordination around Mn(1) is distorted octahedral. The ∠C(9)−Mn(1)−O(12) is 80.2°, which is slightly larger than the average angle of 77.8° found in other reported five-membered manganacycles.[10] The coordination around Mn(2) is also distorted octahedral. The carbonyl ligands coordinated to both metals are linear and are unremarkable in their bond angles and distances. The Mn(1)−Mn(2) distance is 5.32 Å, indicating that no metal−metal bond is present.

The C(9)−C(14) bond length is 1.346(8) Å, indicative of a C−C double bond. The C(29)−N(30) bond length is 1.285(7) Å, the C(11)−N(10) bond length is 1.354(7) Å, and the C(9)−N(10) bond length is 1.443(7) Å, indicating a double bond, a bond that is between single bond and double bond in character, and a single bond, respectively. The C(11)−N(10) bond length in the carbamate is similar to that observed in tungsten and tantalum complexes.[31] The hydrogen atom, H(30), was located directly from the difference electron maps, and the N(30)−H(30) distance is 0.942 Å. The C(29)−C(39) bond length of 1.518(8) Å is as expected for a C−C single bond. The Mn(1)−O(12) bond distance is 2.031(4) Å, and the Mn(2)−O(13) bond length is 2.043(4) Å. These Mn−O lengths are within the range of bond lengths reported for Mn−O(carbonate)[32] and Mn−O(carboxylate)[33] bonds (2.020−2.042 Å) found trans to carbonyl ligands. The bridging carbamato C−O bond lengths are

(30) (a) Atwood, J. D.; Brown, T. L. *J. Am. Chem. Soc.* **1975**, *97*, 3380. (b) Atwood, J. D.; Brown, T. L. *J. Am. Chem. Soc.* **1976**, *98*, 3155.

(31) (a) Chisholm, M. H.; Extine, M. W. *J. Am, Chem. Soc.* **1974**, *96*, 6214. (b) Chisholm, M. H.; Extine, M. W. *J. Am. Chem. Soc.* **1977**, *99*, 792.

(32) Mandal, S. K.; Ho, D. M.; Orchin, M. *Organometallics* **1993**, *12*, 1714.

Table 4. Selected Bond Distances [Å] and Angles [deg] for 12

Mn(1)−C(3)	1.787(8)	Mn(1)−C(2)	1.821(8)
Mn(1)−C(4)	1.839(10)	Mn(1)−C(1)	1.871(9)
Mn(1)−O(12)	2.031(4)	Mn(1)−C(9)	2.074(6)
Mn(2)−C(6)	1.778(7)	Mn(2)−C(5)	1.842(8)
Mn(2)−C(8)	1.849(8)	Mn(2)−C(7)	1.874(9)
Mn(2)−O(13)	2.043(4)	Mn(2)−C(29)	2.046(6)
O(1)−C(1)	1.124(8)	O(2)−C(2)	1.137(8)
O(3)−C(3)	1.149(8)	O(4)−C(4)	1.131(9)
O(5)−C(5)	1.125(8)	O(6)−C(6)	1.156(7)
O(7)−C(7)	1.126(8)	O(8)−C(8)	1.155(8)
O(12)−C(11)	1.264(7)	O(13)−C(11)	1.278(7)
N(10)−C(11)	1.354(7)	N(10)−C(9)	1.443(7)
N(10)−C(21)	1.444(7)	N(30)−C(29)	1.285(7)
N(30)−C(31)	1.446(8)	C(9)−C(14)	1.346(8)
C(3)−Mn(1)−C(2)	89.6(3)	C(3)−Mn(1)−C(4)	94.5(4)
C(2)−Mn(1)−C(4)	93.0(4)	C(3)−Mn(1)−C(1)	88.3(3)
C(2)−Mn(1)−C(1)	94.0(4)	C(4)−Mn(1)−C(1)	172.4(3)
C(3)−Mn(1)−O(12)	173.6(3)	C(2)−Mn(1)−O(12)	90.5(3)
C(4)−Mn(1)−O(12)	91.8(3)	C(1)−Mn(1)−O(12)	85.3(3)
C(3)−Mn(1)−C(9)	99.5(3)	C(2)−Mn(1)−C(9)	170.7(3)
C(4)−Mn(1)−C(9)	84.1(3)	C(1)−Mn(1)−C(9)	88.5(3)
O(12)−Mn(1)−C(9)	80.7(2)	C(6)−Mn(2)−C(5)	92.5(4)
C(6)−Mn(2)−C(8)	88.5(3)	C(5)−Mn(2)−C(8)	92.8(3)
C(6)−Mn(2)−C(7)	92.5(4)	C(5)−Mn(2)−C(7)	173.5(3)
C(8)−Mn(2)−C(7)	91.6(3)	C(6)−Mn(2)−O(13)	176.1(3)
C(5)−Mn(2)−O(13)	87.9(3)	C(8)−Mn(2)−O(13)	95.4(2)
C(7)−Mn(2)−O(13)	86.9(3)	C(6)−Mn(2)−C(29)	93.1(3)
C(5)−Mn(2)−C(29)	84.6(3)	C(8)−Mn(2)−C(29)	177.0(3)
C(7)−Mn(2)−C(29)	90.9(3)	O(13)−Mn(2)−C(29)	83.1(2)
C(11)−O(12)−Mn(1)	114.5(4)	C(11)−O(13)−Mn(2)	129.1(4)
C(11)−N(10)−C(9)	118.3(5)	C(11)−N(10)−C(21)	119.5(5)
C(9)−N(10)−C(21)	122.2(5)	C(29)−N(30)−C(31)	129.6(6)
O(1)−C(1)−Mn(1)	177.2(8)	O(2)−C(2)−Mn(1)	175.8(8)
O(3)−C(3)−Mn(1)	174.5(7)	O(4)−C(4)−Mn(1)	178.0(8)
O(5)−C(5)−Mn(2)	175.9(7)	O(6)−C(6)−Mn(2)	178.1(8)
O(7)−C(7)−Mn(2)	175.4(8)	O(8)−C(8)−Mn(2)	174.5(6)
C(14)−C(9)−N(10)	116.3(5)	C(14)−C(9)−Mn(1)	136.9(5)
N(10)−C(9)−Mn(1)	106.7(4)	O(12)−C(11)−O(13)	122.9(6)
O(12)−C(11)−N(10)	119.1(6)	O(13)−C(11)−N(10)	118.0(6)
C(9)−C(14)−C(15)	128.8(6)	N(30)−C(29)−C(39)	116.2(6)
N(30)−C(29)−Mn(2)	117.2(5)	C(39)−C(29)−Mn(2)	126.4(5)
C(40)−C(39)−C(29)	115.1(6)		

1.264(7) and 1.278(7) Å for C(11)−O(12) and C(11)−O(13), respectively. These C−O bond lengths are shorter than expected for a C−O single bond (∼1.34 Å) and longer than expected for a C−O double bond (∼1.20 Å). The bond distances in the bridging carbamate suggest delocalization throughout the carbamate. The spectroscopic data are consistent with the structure of **12**, including the IR spectrum, which shows multiple terminal carbonyl bands from 2095 to 1936 cm^{-1} and a band at 1554 cm^{-1} from the C═N stretch.

Since **12** (containing a bridging carbamate) is a very unexpected product based on the known Mn chemistry, it is of interest to determine the mechanism of its formation. Complex **12** was not present in the initial reaction mixture. It was formed when the reaction mixture in a dichloromethane/hexane solution was cooled in dry ice over several days. A number of experiments were carried out to explore the mechanism of formation of **12**. The question is the source of the "extra" O in the μ-carbamate. The original reaction was performed under an inert atmosphere, while the workup was not. The reaction conditions investigated are summarized in Table 5.

Table 5. Reaction Conditions Employed to Elucidate the Mechanism of Formation of 12

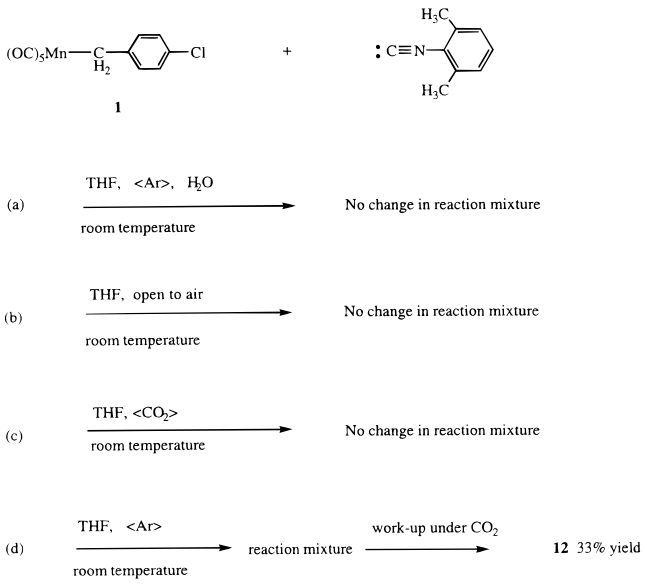

The product mixtures from H_2O, CO_2, and air added to the reactants had the same composition as the reaction mixture obtained under an argon atmosphere as determined by IR spectroscopy. This indicates that none of these species react with the starting materials to give **12**. However, if the product mixture is placed under a carbon dioxide atmosphere over days, the yield of **12** increases significantly, from 6% to 33%. This indicates that the dimer is formed slowly and that CO_2 is required. The IR spectrum after the CO_2 exposure indicates that all of the acyl **11** has been consumed, suggesting that **11** is involved in the production of **12**. Also, the yield of **12** is similar to the yield of **11** calculated from the ^1H NMR of the initial reaction mixture prior to workup. From these results the mechanism for the formation of **12** is proposed in Scheme 3.

The first step is the formation of **11**. Over time, **11** decarbonylates and isocyanide insertion occurs, forming a coordinatively unsaturated mono(iminoacyl) intermediate **13**. Manganese mono(iminoacyl) complexes have been proposed as highly reactive intermediates in other systems.[11] This mono(iminoacyl) intermediate, **13**, reacts via attack on electrophilic CO_2 by the imino nitrogen lone pair giving **14**, which is not spectroscopically observable. Intermolecular attack by **14** on the metal center of another unsaturated mono(iminoacyl) intermediate, **13**, occurs followed by an intramolecular attack of the manganese center by the oxygen of CO_2, thus closing the ring. Intermolecular attack by the CO_2 oxygen may occur before intramolecular attack; otherwise one would expect the isolation of a monomeric kinetic product, a carbamate metallacycle, **15**. It may be that intramolecular attack does occur reversibly giving **15**, but that only proton transfer leads to a thermodynamically stable product, the dimer **12**. Presumably, **12** is not formed in the reaction conducted in the presence of CO_2 because **13** reacts faster with isocyanide rather than with CO_2**.** Currently, efforts in our lab are ongoing using manganese acyl complexes with various aromatic isocyanides to investigate their reactions with CO_2, CS_2, and other cumulenes.

(33) (a) Herrmann, W. A.; Schweizer, I.; Skell, P. S.; Ziegler, M. L.; Wiedenhammer, K.; Nuber, B. *Chem. Ber.* **1979**, *112*, 2423. (b) Cotton, F. A.; Darensbourg, D. J.; Kolthammer, B. W. S. *Inorg. Chem.* **1981**, *20*, 1287.

Scheme 3

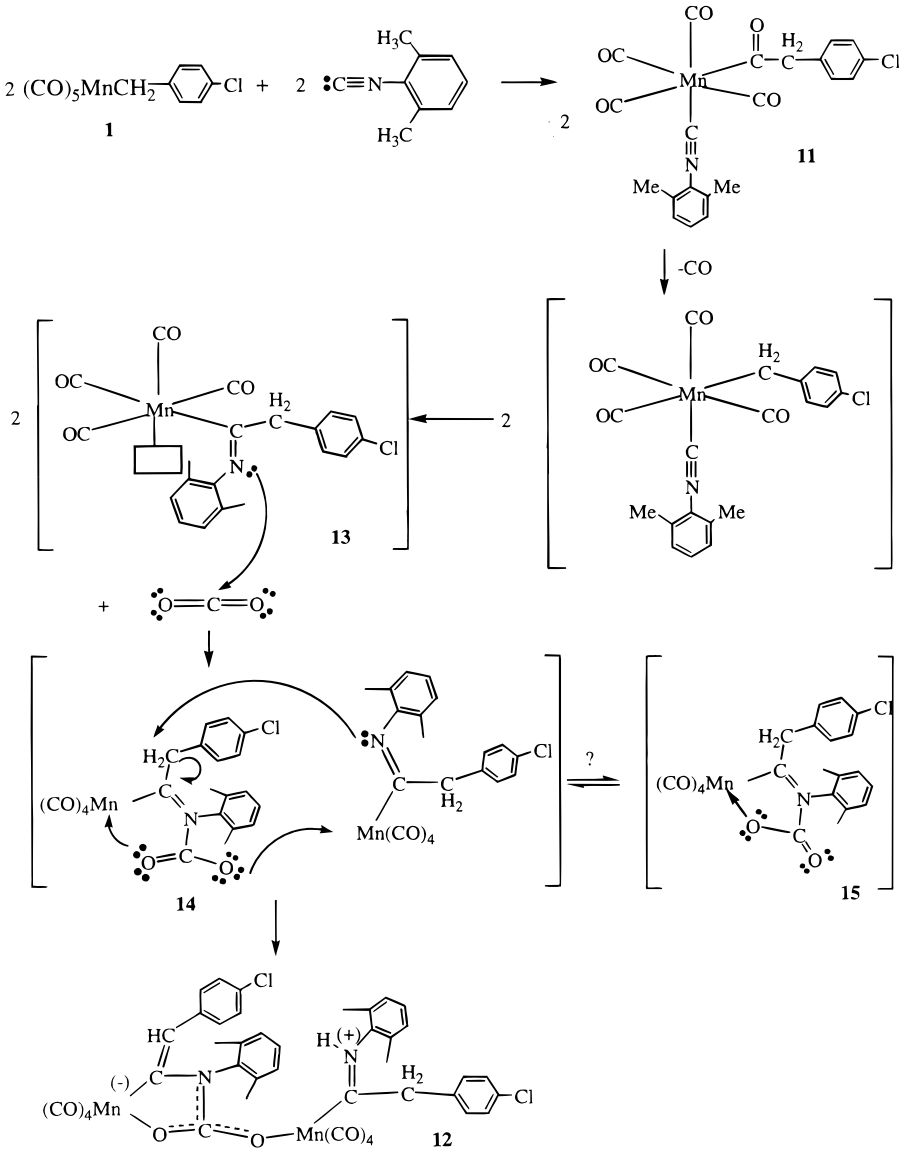

2.4. Summary. The complex product mixtures, found in the described reactions with xylyl isocyanide, provide difficult circumstances in which to isolate the various products. Alkylmanganesepentacarbonyls reacted with xylyl isocyanide in the presence of PdO and produced several products distinct from those isolated from reaction with the smaller *p*-tolyl isocyanide, including the first tris(iminoacyl) manganacycle. It was also found that when a manganese acyl complex containing a terminal xylyl isocyanide was exposed to CO_2, a unique dimanganese complex, which is linked by a carbamato bridge, was formed.

3. Experimental Section

All reactions were performed under argon using standard Schlenk techniques[34] unless otherwise noted. Infrared spectra were recorded on a Perkin-Elmer 1600 Series FTIR spectrophotometer. IR cells were 1.0 mm solution cells with NaCl windows. ^{1}H and ^{13}C NMR data were recorded using a Bruker AM-250 spectrometer, and the chemical shifts are given in ppm downfield from tetramethylsilane. Elemental analyses were performed by Chemisar Laboratories, Guelph, Canada. Mass spectra were recorded on a VG 30−250 quadrupole mass spectrometer with an Ion Tech saddle field ion (FAB) gun. The gun was operated employing argon as the bombarding gas with an ion current of 1 mA and an ion gun potential of 8 kV. The typical matrix was 3-nitrobenzyl alcohol. The instrument was scanned for positive ions from 25 to 1200 Da with a scan time of 4.9 s/scan. Melting points were determined on a Mel-Temp melting point apparatus and are uncorrected.

All solvents were dried prior to use employing standard techniques. PdO was purchased from Aldrich and used as received. Dimanganese decacarbonyl was purchased from Strem Chemical Co. and used as received. Xylyl isocyanide was purchased from Fluka and used without further purification. $(CO)_5MnCH_2C_6H_4$-*p*-Cl, **1**, was prepared according to the published method.[12]

3.1. General Conditions for Reactions in the Presence of PdO. Complex **1** and xylyl isocyanide (1:2 mol ratio) were placed in a flask. A catalytic amount of PdO (approximately 0.02 g) was added. Toluene was injected into the flask, and the solution was stirred at least overnight. The color of the mixture changed from yellow to red. The solvent was removed in vacuo, and complexes **2**−**6** were isolated as described below.

(34) Shriver, D. F.; Drezdzon, M. A. *The Manipulation of Air-Sensitive Compounds*, 2nd ed.; Wiley: New York, 1986.

Isolation of $Mn_2(CO)_9$(CN-xylyl) (2). Complex **1** (0.822 g, 2.57 mmol), xylyl isocyanide (0.680 g, 5.18 mmol), and PdO (approximately 0.02 g) were placed in a flask and stirred in 30 mL of toluene for 4 days. A 15 mL sample of the solution was removed from the flask, and the solvent was removed in vacuo. A silica gel column was prepared, and the residue was eluted from 15% THF in hexane. The first band was yellow. Solvent was removed via rotary evaporation. Hexane was added and the solution cooled to 0 °C. Complex **2** (0.0441 g, 8.7% yield) was isolated as a yellow solid. The spectroscopic data compared favorably to that previously reported.[20]

Isolation of $(CO)_3$(CN-xylyl)Mn[C(=N-xylyl)C(=N-xylyl)-$CH_2C_6H_4$-*p*-Cl] (3). Complex **3** was isolated from reaction mixtures with and without PdO. **1** (0.822 g, 2.57 mmol) was stirred in the presence of PdO (approximately 0.02 g) and xylyl isocyanide (0.680 g, 5.18 mmol) in 30 mL of toluene for 4 days. The solvent was removed, and the residue was chromatographed on two successive silica gel columns and eluted with 15% THF/hexane. The first red band was isolated from each column, and the solvent was removed. THF was added, and the mixture was cooled to 0 °C, affording **3** (0.148 g, 9% yield) as a red solid. Suitable crystals of **3** for X-ray analysis were grown from CH_2Cl_2/hexane in an NMR tube at 0 °C.

Spectral Data for 3. IR ($CHCl_3$): cm^{-1} C≡N 2121 (s), C≡O 2008 (vs), 1950 (vs), 1925 (vs). ^1H NMR ($CDCl_3$), ppm: 7.21−6.92 (m, Ph, 13H), 3.59 (AB quartet, J = 12.25 Hz, CH_2, 2H), 2.25 (s, Mn−N-xylyl−CH_3, 3H), 2.24 (br, Mn−C−N-xylyl-CH_3, 6H), 2.18 (s, terminal-xylyl−CH_3, 6H), 2.07 (s, Mn−N-xylyl−CH_3, 3H). ^{13}C NMR ($CDCl_3$), ppm: 221.1 (CO), 219.7 (CO), 215.0 (CO), 206.1 (Mn−terminal-CNR), 187.9 (Mn−C), 179.1 (Mn−N−C), 153.1−122.9 (singlets, Ph), 33.5 (CH_2), 22.7−18.4 (m, CH_3). Mass spectrum: 658 (M^+ + 1), 574 (M^+ − 3CO). Anal. Found: C, 67.2; H, 5.18. Calcd for $C_{37}H_{33}$: C, 67.5; H, 5.05.

Isolation of $(CO)_4$(CN-xylyl)Mn[C(=N-xylyl)C(=N-xylyl)-$CH_2C_6H_4$-*p*-Cl] (4). The experimental details can be found above in the preparation of **2**. Complex **4** (0.0041 g, 0.5% yield) was isolated from an orange chromatography band in which the solvent was removed and orange solids were isolated.

Spectral Data for 4. IR ($CDCl_3$), cm^{-1}: C≡N 2112 (s), C≡O 2016 (s), 1996 (s), 1973 (s), 1949 (vs, br), C=N 1620 (m), 1601 (m). ^1H NMR ($CDCl_3$), ppm: 7.16−6.14 (m, Ph, 13H), 3.51 (s, CH_2, 2H), 2.31 (s, CH_3, 6H), 2.11 (s, CH_3, 6H), 2.07 (s, CH_3, 6H). No analysis could be obtained due to the extremely small amount of material isolated.

Isolation of $(CO)_4$Mn[C{=CH(C_6H_4-*p*-Cl)}N-xylyl)C-(NH-xylyl)] (5). The experimental details are described above in the preparation of **2**. Complex **5** (0.0252 g, 3.5% yield) was isolated from the fifth chromatography band. The solvent was removed and washed with hexane. The residue was recrystallized from CH_2Cl_2 affording **5** as colorless crystals.

Spectral Data for 5. IR ($CHCl_3$), cm^{-1}: N−H 3296 (w), C≡O 2066 (m), 1983 (vs), 1973 (vs), 1945 (s). ^1H NMR ($CDCl_3$), ppm: 7.30−7.14 (m, Ph, 10H), 7.04 (s, br, NH, 1H), 6.40 (s, C=CH, 1H), 2.36 (s, CH_3, 6H), 2.34 (s, CH_3, 6H). ^{13}C NMR ($CDCl_3$), ppm: 140−117 (m, Ph), 18.6 (s, CH_3), 18.0 (s, CH_3). Mass spectrum: 554 (M^+), 443 (M^+ − 4CO). Anal. Found: C, 62.21; H, 4.61. Calcd for $C_{29}H_{24}$: C, 62.77; H, 4.36.

Isolation of $(CO)_4$Mn[C(=N-xylyl)C(=N-xylyl)-$CH_2C_6H_4$-*p*-Cl] (6). A green fraction of the chromatography column described above in the preparation of **2** was taken, and the solvent was removed giving **6** (0.062 g, 2.7% yield)) as a green solid.

Spectral Data for 6. IR ($CDCl_3$), cm^{-1}: C≡O 2068 (s), 1991, (vs), 1977 (vs), 1955 (vs). ^1H NMR ($CDCl_3$), ppm: 7.24−6.76 (m, Ph, 13H), 3.94 (s, CH_2, 2H), 2.15 (s, CH_3, 6H), 2.00 (s, CH_3, 6H), 1.88 (s, CH_3, 6H). ^{13}C NMR ($CDCl_3$), ppm: 132−122 (singlets, Ph), 18.7 (s, CH_3), 18.4 (s, CH_3), 17.8 (s, CH_3). Mass spectrum: 686 (M^+ + 1), 575, (M^+ − 4CO). Anal. Found: C, 65.10; H, 5.32. Calcd for $C_{38}H_{33}$: C, 66.52; H, 4.85.

Isolation of $(CO)_3(CN\text{-}xylyl)_2MnC(O)CH_2C_6H_4$-*p*-Cl] (9). The reaction of **1** (0.785 g, 2.46 mmol) with xylyl isocyanide (0.646 g, 4.92 mmol) was run in 20 mL of THF with PdO (0.02 g). The mixture was stirred for 22 h, and the solvent was removed in vacuo. Two chromatographies were performed. The first was on silica gel with 5% THF in hexane. An orange-yellow fraction was rechromatographed on silica gel with 25% hexane in THF, affording an orange band. The solvent was removed, hexane/CH_2Cl_2 was added, and the mixture was cooled to 0 °C. Yellow solids of **9** (0.3067 g, 29% yield) were isolated.

Spectral data for 9. IR (THF), cm^{-1}: C≡N 2161 (m), 2124 (m), C≡O 2010 (vs), 1966 (vs), 1944 (vs), C=O 1628 (m, br). ^1H NMR ($CDCl_3$), ppm: 7.30−7.00 (m, Ph, 10H), 4.20 (s, CH_2, 2H), 2.41 (s, CH_3, 12H). ^{13}C NMR ($CDCl_3$), ppm: 137−117 (singlets, Ph), 70.2 (s, CH_2), 18.6 (s, CH_3), 18.0 (s, CH_3). Mass spectrum: 555 (M^+), 471 (M^+ − 3CO). Anal. Found: C, 62.47; H, 4.27. Calcd for $C_{29}H_{24}$: C, 62.77; H, 4.36.

3.2. General Reaction Conditions without PdO. Complex **1** and xylyl isocyanide (1:1 mol ratio) were placed in a reaction flask. THF was added, and the mixture was allowed to stir overnight. The color of the solution changed from yellow to red, and the solvent was removed in vacuo. Isolation of the greatest yields of complexes **3**, **11**, and **12** from this reaction is described below.

Isolation of *fac*-$(CO)_3$(CN-xylyl)Mn[C(=N-xylyl)C(=N-xylyl)$CH_2C_6H_4$-*p*-Cl] (3). Xylyl isocyanide (0.400 g, 3.05 mmol) was stirred with **1** (0.972 g, 3.04 mmol) in 30 mL of THF for 18 h. After solvent removal, the residue was chromatographed on a silica gel column with a 1:9 Et_2O/hexane solution as the eluent. An orange band was isolated and rechromatographed employing the same conditions. Again, an orange band was isolated. The solvent was removed, and the red solid **3** was recrystallized from hexane (0.0773 g, 11.6% yield). Spectroscopic data were given earlier in this report.

Isolation of $(CO)_4$(CN-xylyl)MnC(O)$CH_2C_6H_4$-*p*-Cl (11). Complex **1** (1.51 g, 4.71 mmol) was stirred in 20 mL of THF with xylyl isocyanide (0.619 g, 4.72 mmol) for 19 h. After solvent removal, the residue was recrystallized from CH_2Cl_2/hexane at 0 °C. Pale yellow needles of **11** (0.037 g, 2.0% yield) were isolated.

Spectral Data for 11. IR (THF), cm^{-1}: C≡N 2164 (m), C≡O 2065 (s), 2004 (sh), 1985 (vs), 1972 (sh), C=O 1637 (m). ^1H NMR ($CDCl_3$), ppm: 7.24−7.01 (m, Ph, 7H), 4.15 (s, CH_2, 2H), 2.42 (s, CH_3, 6H). Anal. Found: C, 56.27; H, 3.40. Calcd for $C_{21}H_{15}$: C, 55.83; H, 3.35.

Isolation of $(CO)_4$Mn[C{=CH(C_6H_4-*p*-Cl)}N-(xylyl)C-(O)OMn$(CO)_4$[C(=NH-xylyl)$CH_2C_6H_4$-*p*-Cl]] (12). A THF solution of **1** (0.590 g, 1.85 mmol) and xylyl isocyanide (0.242 g, 1.85 mmol) was stirred for 22 h. The solvent was removed in vacuo. The flask was filled with CO_2, and CH_2Cl_2/hexane was added via syringe. The sealed flask was cooled to 0 °C and afforded the yellow solid **12** (0.273 g, 33.1% yield). Crystals of **12** suitable for X-ray analysis were grown from CH_2Cl_2/hexane at 0 °C.

Spectral Data for 12. IR ($CHCl_3$), cm^{-1}: C≡O 2095 (m), 2077 (m), 2025 (sh), 2007 (vs), 1988 (s), 1936 (s), C=N 1554 (m). ^1H NMR ($CDCl_3$), ppm: 7.2−6.4 (m, Ph, N−H, 15 H), 6.04 (s, C=CH, 1H), 4.01 (s, CH_2, 2H), 2.08 (s, CH_3, 6H), 1.75 (s, CH_3, 6H). ^{13}C NMR ($CDCl_3$), ppm: 142−116 (singlets, Ph), 50.9 (s, CH_2), 17.8 (s, CH_3), 17.5 (s, CH_3). Mass spectrum: 891 (M^+), 778 (M^+ − 4CO), 750 (M^+ − 5CO), 722 (M^+ − 6CO), 666 (M^+ − 8CO). Anal. Found: C, 55.5; H, 3.9. Calcd for $C_{41}H_{30}$: C, 55.2; H, 3.4.

3.3. X-ray Diffraction Studies of 3, 6, and 12. Crystals of **3**, **6**, and **12** suitable for X-ray diffraction were obtained from CH_2Cl_2/hexane. For room-temperature X-ray examination and

data collection, each crystal was coated with a light film of epoxy resin and mounted on a glass fiber. Intensity data for **3** and **12** were collected using graphite-monochromated Cu Kα radiation, while **6** was analyzed using graphite-monochromated Mo Kα radiation.

Lattice parameters for **3** and **12** were obtained by least-squares refinement of the angular settings from 25 reflections lying in a 2θ range of 10−60°. Intensity data for **3** was collected using $\theta-2\theta$ scans in the range $4° < 2\theta < 120°$. For **12**, intensity data were collected using $\theta-2\theta$ scans in the range $4° < 2\theta < 115°$. Lattice parameters for **6** were obtained by least-squares refinement of the angular information from 201 reflections measured at 0.3° increments of ω with three different 2θ and ϕ values and a detector-to-crystal distance of 4.959 cm. Intensity data for **6** were collected as 10 s data frames measured at 0.3° intervals of ω covering nearly one hemisphere of intensity data with a maximum 2θ value of 56.62°. The data for all three compounds were corrected for decay, Lorentz, and polarization effects. Data for **3** and **6** were also corrected for absorption effects (**3**: based on measured ψ scans, correction: min transmission 0.7645, max transmission 1.0000; **6**: semiempirical absorption correction using SADABS, correction: min transmission 0.7663, max transmission 0.9280).[35]

Structures for **3**, **6**, and **12** were solved by a combination of direct methods using SHELXTL v5.03[36] and the difference Fourier technique and were refined by full-matrix least-squares on F^2 (data for **6** were used out to 0.8 Å resolution). Non-hydrogen atoms were refined with anisotropic displacement parameters. Weights were assigned as $w^{-1} = \sigma^2(F_o^2) + (aP)^2 + bP$ where $P = 0.33333F_o^2 + 0.66667F_c^2$ and $a = 0.0930$, $b = 23.9669$ for **3**, $a = 0.0310$, $b = 1.1469$ for **6**, and $a = 0.1101$, $b = 1.2962$ for **12**. An extinction correction of the form $k[1+0.001(\chi F_c^2\lambda^3)]/\sin(2\theta)]^{-1/4}$ was applied (**3**, $k = 0.28507$ and $\chi = 0.00042(7)$; **12**, $k = 0.4638$ and $\chi = 0.00042(11)$). Aromatic and methylene H atom positions for **6** were calculated on the basis of a geometric criterion, while methyl H atom positions for **3** and **6** were calculated after the location of one H atom from the electron density map. All H atom positions for **3** and **6** were allowed to ride on their respective atoms. All methyl groups in **6** had disordered hydrogen positions, and occupancies were fixed at 0.5. In **12**, the H atom positions were calculated on the basis of a geometric criterion and allowed to ride on their respective atoms with the exception of H30. H30 was located directly from the difference electron density map, and its position was allowed to refine. H atom isotropic temperature factors for all three structures were defined as $U(C)*a = U(H)$ where $a = 1.5$ for methyl hydrogens and $a = 1.2$ for the remaining hydrogens. Compound **12** packs in the crystalline lattice with a badly disordered CH_2Cl_2 (occupancy = 0.5). The solvent contribution from the reflection data was subtracted out using SQUEEZE,[37] and the modified reflection data were subsequently used in the final stages of refinement. The three structural refinements converged with crystallographic agreement factors summarized in Table 1.

3.4. Molecular Modeling of 3. Modeling was carried out using Insight II (version 95.2) and Discover (version 4.0), both from Molecular Simulations Inc. The ESFF force field was used, as it had suitable parameters for the organometallic complex.[38,39]

Energy minimization of the complex began with coordinates obtained from X-ray crystallography. The minimization protocol was a cascade of increasingly more accurate methods starting with the steepest descents method and continuing through conjugate gradients to the quasi-Newton−Raphson method using the Broyten, Fletcher, Goldfarb, and Shanno (BFGS) approach. At each step the maximum number of steps used for each method was 250 to a final convergence of 0.001. No cutoff was used for calculating nonbonded interactions. A constant dielectric constant of 1.0 was used.

Molecular dynamics simulations were carried out at a constant temperature and volume with no nonbonded cutoff and a dielectric constant of 1.0. The system was heated in 100 steps from an initial temperature of 298 K to the target temperature. Temperature was maintained by velocity scaling. After heating, data were collected over 50 000 steps (50 ps) at 10 fs intervals. The system reached equilibrium very quickly, as evidenced by the stability of temperature and potential energy through the course of the simulation (data not shown).

Acknowledgment. Mr. Jim Carlson obtained the mass spectra. We thank E.M. Science for a gift of silica gel. T.M.B. is grateful for financial support in the form of a Quantum Chemical (now Millennium Petrochemicals) fellowship and from a scholarship from the Research Scholars program in the Department of Chemistry at the University of Cincinnati. J.A.K.B. sincerely thanks Dr. Charles Campana (Bruker AXS Inc.) and Dr. Ewa Skrzypczak-Jankun (University of Toledo) for assistance in using the CCD diffractometer system for **6**. Data were collected through the Ohio Crystallographic Consortium, funded by the Ohio Board of Regents 1995 Investment Fund (CAP-075), located at the University of Toledo, Instrumentation Center in A&S, Toledo, OH 43606. The authors thank Prof. John S. Ricci and Mr. Jeffrey B. Fortin of the University of Southern Maine, Portland, ME, for help in collecting crystallographic data.

Supporting Information Available: Lists of H atom coordinates and isotropic thermal parameters, anisotropic thermal parameters for other atoms, bond distances, bond angles, and torsion angles are available for **3**, **6**, and **12** as well as molecular modeling graphs depicting torsion angles versus time for all three xylyl isocyanides in **3**.

OM9903644

(35) Data for **3** were collected on a Rigaku AFC5R rotating anode diffractometer. The TEXSAN suite of programs were used for data collection and data processing, Molecular Structure Corp.: Woodlands, TX. Data for **6** were collected on a Siemens SMART 1K CCD diffractometer. The SMART v4.05 and SAINT v4.05 programs were used for data collection and data processing, Siemens Analytical X-ray Instruments, Inc.: Madison, WI. SADABS was used for the application of a semiempirical absorption correction, G. M. Sheldrick, University of Goettingen, Germany. Data for **12** were collected on a Siemens P4 diffractometer. The XSCANS suite of programs were used for data collection and data processing, Siemens Analytical X-ray Instruments, Inc.: Madison, WI.

(36) SHEXLXTL v5.03 was used for the structure solution and generation of figures and tables, Siemens Analytical X-ray Instruments, Inc.: Madison, WI. Neutral-atom scattering factors were used as stored in SHELXTL v5.03.

(37) SQUEEZE is a routine implemented in PLATON-92, which allows solvent contributions to be eliminated from the reflection data. A. L. Spek, University of Utrecht, Utrecht, The Netherlands.

(38) Forcefield-Based Simulations; Molecular Simulations Inc.: San Diego, April 1997.

(39) Shi, S.; Yan, L.; Shaulski, J.; Thacher, T. Manuscript in preparation.